Metal-free ionic liquids serve as integrated catalyst-solvent systems for green H_2S oxidation to sulfur by O_2

Mingzhen Shi[a,b], Hongchao Lan[a], Hailong Ning[a], Xiaomin Zhang[a,c]*, Xingbang Hu[a], Youting Wu[a]*

[a] State Key Laboratory of Coordination Chemistry, School of Chemistry, Nanjing University, Nanjing 210023, PR China.

[b] Key Laboratory of Synthetic and Natural Functional Molecule of the Ministry of Education, College of Chemistry & Materials Science, Northwest University, Xi'an 710127, PR China.

[c] State Key Laboratory of Coordination Chemistry, Suzhou Key Laboratory of Green Intelligent Manufacturing of New Energy Materials and Devices, the Institute of Green Chemistry and Engineering, Nanjing University, Jiangsu 215163, P.R. China.

*Corresponding author. Email: xmzhang@nju.edu.cn; ytwu@nju.edu.cn.

List of Contents:

1. Materials

H_2S and O_2 (99.99 mol% purity) were purchased from Nanjing Chuangda Gas Co., Ltd, China. The abbreviations, purity, and suppliers of the reagents used are listed in **Table S1**, and all reagents were used without further purification.

2. Methods

2.1 Methodology for Evaluating the Conversion Rate of H_2S

The conversion rate of H_2S is determined based on the residual gas pressure in the reactor after the reaction, calculated as follows:

Assume that upon completion of the reaction, the total pressure of the residual gas within the reaction vessel is P (in bar), where the partial pressures of H_2S and O_2 are x and y, respectively:

$$P = x + y \tag{S1}$$

Therefore, the amounts of residual H_2S and O_2 in the gas phase are:

$$n_{H_2S} = \frac{xV_g}{RT} \tag{S2}$$

$$n_{O_2} = \frac{yV_g}{RT} \tag{S3}$$

In Equations (S2) and (S3), V_g is the gas-phase volume of the reactor, calculated as the total reactor volume minus the volume of the IL. R is the ideal gas constant (83.14472 mL·bar/(K·mol)), and T is the reaction temperature in Kelvin. Assuming the solubility of the reaction products (sulfur and water) in H_2S and O_2 is negligible, the amounts of H_2S and O_2 in the liquid phase can be expressed as:

$$n_{H_2S} = f_1(x)m_{IL} \tag{S4}$$

$$n_{O_2} = f_2(y)m_{IL} \tag{S5}$$

In Equations (S4) and (S5), f_1 and f_2 represent the functional relationships between the solubility (on a molality basis) of H_2S and O_2 in ILs and their respective partial pressures, while m_{IL} denotes the mass of the IL sample. The solubility measurement method is detailed in **"Section 2.2 Single-component Gas Absorption Measurements"**.

Assuming no side reactions occur, the residual amounts of H_2S and O_2 in the reactor follow the stoichiometric ratio:

$$n_{H_2S,g} + n_{H_2S,l} = 2(n_{O_2,g} + n_{O_2,l}) \tag{S6}$$

By combining Equations (S2)–(S6), equation (S7) was obtained:

$$\frac{P_1V}{RT} + f_1(x)m_{IL} = 2\left[\frac{P_2V}{RT} + f_2(y)m_{IL}\right] \quad \text{(S7)}$$

Subsequently, solving the simultaneous equations (S1) and (S7) yields x and y. The H_2S conversion can then be calculated using Equation (S8):

$$\alpha_{H_2S} = 1 - \frac{n_{H_2S,g} + n_{H_2S,l}}{n_{H_2S,t}} \quad \text{(S8)}$$

where $n_{H_2S,t}$ represents the total amount of H_2S initially injected (6 mmol).

2.2 Single-component Gas Absorption Measurements

As shown in **Fig. S3**, the absorption device consists of two glass chambers. The larger chamber is used as a gas reservoir for storing gas, while the smaller one is used as an equilibrium cell and equipped with a magnetic stirrer, where the gas absorption in ILs takes place. The temperature of the two chambers is controlled by a water bath with an uncertainty of 0.1 °C. The pressures in the two chambers are measured by two pressure sensors, which are connected to a Numerical Instrument to detect the pressure changes on-line.

Take the measurement of H_2S uptake capacity in ILs as an example. In a typical run, a known mass of IL sample was added to the equilibrium cell and then two chambers were vacuumed. A certain amount of H_2S gas was fed into the gas reservoir from the gas cylinder, and the pressure of the gas reservoir was recorded as P_1. Open the valve between the two chambers and put a certain amount of H_2S gas from the gas cylinder into the equilibrium cell. Equilibrium was achieved when the pressure of the equilibrium cell kept unchanged for 1 h. The pressures of the gas reservoir and equilibrium cell were denoted as P_2 and P_3, respectively. Then, the gas solubility at an equilibrium pressure of P_3 can be calculated as follows:

$$n_{gas} = \rho_{gas}^{P_1,T}V_1 - \rho_{gas}^{P_2,T}V_2 - \rho_{gas}^{P_3,T}\left(V_2 - \frac{m_{IL}}{\rho_{IL}}\right) \quad \text{(S9)}$$

where n_{gas} is the amount of gas dissolved (mol), $\rho_{gas}^{P_i,T}$ refers to the gas density at P_i and T (mol/L) (data obtained from the NIST Chemistry WebBook [1]), V_1 and V_2 are the volumes of the gas reservoir and equilibrium cell respectively (mL), m_{IL} is the mass of the sample (g), and ρ_{IL} is the density of the sample (g/mL). The values of V_1 and V_2 were calibrated using N_2 as the probing gas. The gas solubility at elevated pressures was determined by injecting enhanced amounts of H_2S gas into the equilibrium cell.

The solubilities of O_2 were tested in the same way as H_2S.

2.3 Thermodynamic modeling of H_2S absorption

The dissolution behavior of H_2S in the ILs investigated in this work was modeled using the reaction equilibrium thermodynamic model (RETM), which is proposed based on the Henry's law and reaction equilibrium equation. For the superbase-derived IL [DBUH]Im, a 1:1 complexation mechanism with H_2S was adopted, and the detailed formulation has been previously reported by our research group [2]. For the remaining ILs, a 2:1 (IL:H_2S) interaction stoichiometry was employed in the thermodynamic fitting, and the corresponding derivation process is as follows:

The absorption of H_2S in the investigated IL can be divided into two steps: (1) H_2S transfer from gas phase to liquid phase; (2) H_2S react with the IL to form H_2S-IL complexes. Then the reaction of H_2S with ILs can be expressed by the following equation:

$$H_2S(g) \rightarrow H_2S(l) \tag{S10}$$

$$H_2S(l) + 2IL(l) \rightarrow H_2S-2IL(l) \tag{S11}$$

where g and l in Equations S10 and S11 represent the existing states (gas and liquid, respectively) of a species.

The first step is the physical absorption process, described by Henry's law

$$P = H \cdot m_{H_2S} \tag{S12}$$

where P represents the equilibrium pressure of H_2S in gas phase, H is the Henry constant of H_2S in liquid phase, and m_{H_2S} is the molarity of free H_2S in liquid phase.

The second step is the chemical absorption process, and can be depicted by the reaction equilibrium equation

$$K^{\circ} = \frac{m_{H_2S-2IL}}{m_{H_2S} \cdot {m_{IL}}^2} \tag{S13}$$

where K° is the reaction equilibrium constant for Equation S11, m_{H_2S-2IL} is the molality of the H_2S-IL complex in liquid phase, and the m_{IL} is the molality of free IL in liquid phase.

The overall absorption of H_2S in the investigated IL can be denoted as follows

$$H_2S(g) + 2IL(l) \rightarrow H_2S-2IL(l) \tag{S14}$$

which can be expressed by the reaction equilibrium equation

$$K = \frac{m_{H_2S-2IL}}{P \cdot {m_{IL}}^2} \tag{S15}$$

where K is the reaction equilibrium constant for Equation S14. The material balance equations of H_2S and IL are shown in Equations S16 and S17, respectively.

$$m_{H_2S}^{t} = m_{H_2S} + m_{H_2S-2IL} \tag{S16}$$

$$m_{IL}^{t} = m_{IL} + 2m_{H_2S-2IL} \tag{S17}$$

where $m_{H_2S}^{t}$ is the total solubility of H_2S in mol·kg^{-1} in the investigated IL, and m_{IL}^{t} is the initial molality of IL in mol·kg^{-1} in the liquid phase.

Combining Equation S12 and Equations S15-17 resulted in Equation S18 after simple derivation

$$m_{H_2S}^{t} = \frac{4KPm_{IL}^{t} + 1 - \sqrt{8KPm_{IL}^{t} + 1}}{8KP} + \frac{P}{H} \tag{S18}$$

Equation S18 was then used for correlating the solubility of H_2S in the investigated ILs.

The expression obtained by correlating the solubility data of H_2S in different ILs is shown in **Table S2**. For the solubility of O_2 in these ILs, a linear fitting method was applied, and the resulting fitting expressions are also summarized in **Table S2**.

3. Figs. S1 to S5.

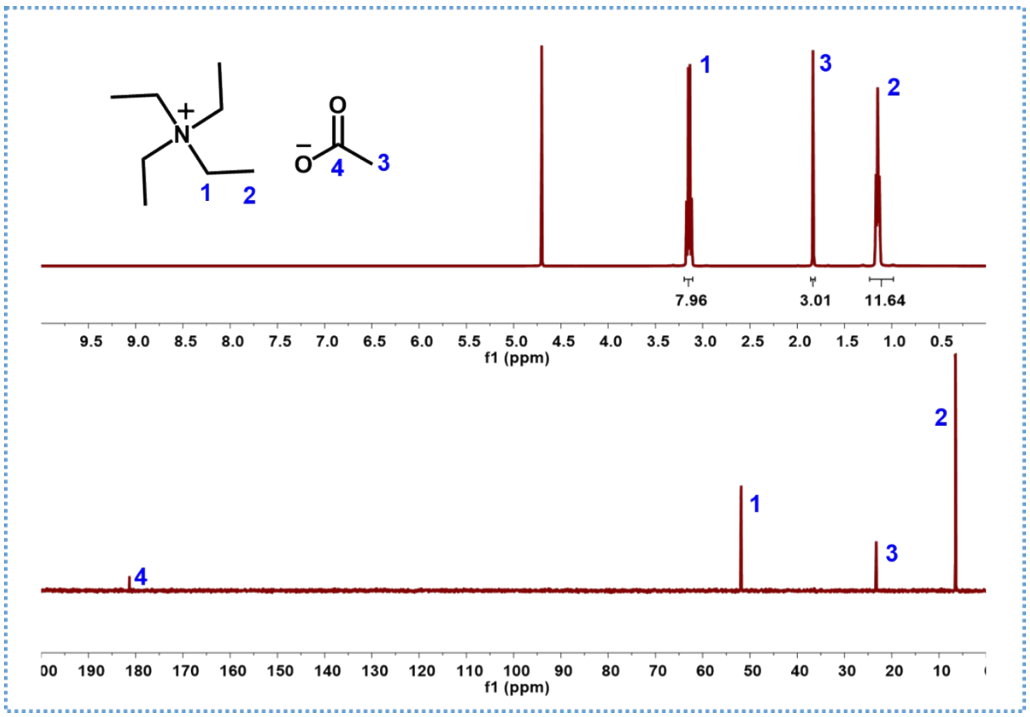

Fig. S1. ^{1}H and ^{13}C NMR spectra of $N_{2222}Ac$.

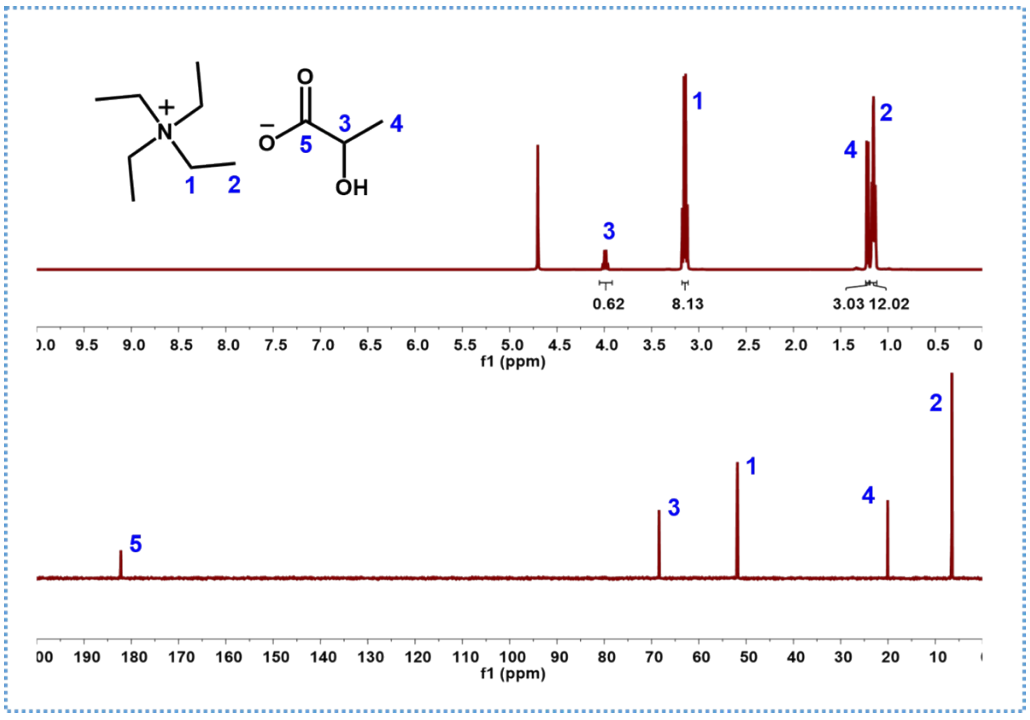

Fig. S2. ^{1}H and ^{13}C NMR spectra of $N_{2222}L$.

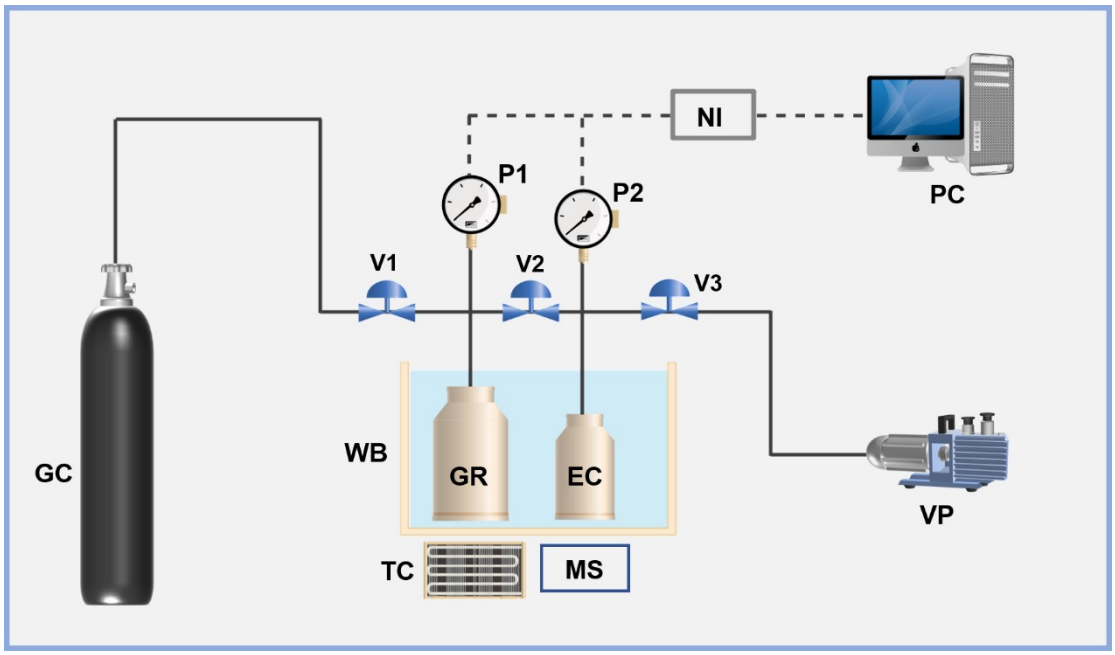

Fig. S3. Apparatus for the determination of gas solubility. (GC – gas cylinder; V1, V2, V3 – valves; WB – water bath; GR – gas reservoir; EC – equilibrium cell; TC – thermal controller; MS – magnetic stirrer; VP – vacuum pump; P1, P2 – pressure transducer; NI – numerical instrument; PC – personal computer).

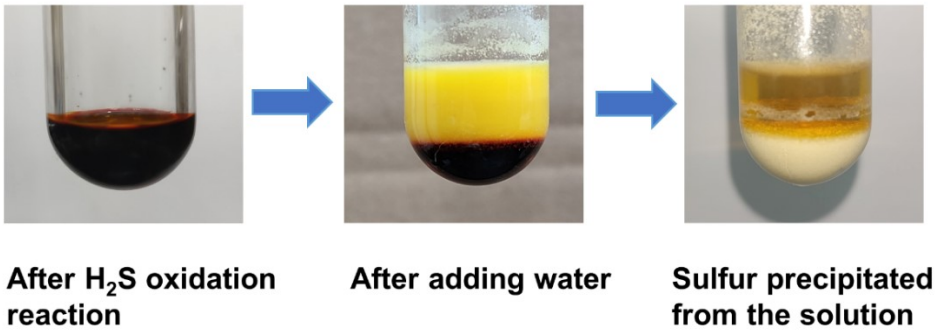

Fig. S4. Sulfur precipitation upon completion of H_2S oxidation in EmimAc.

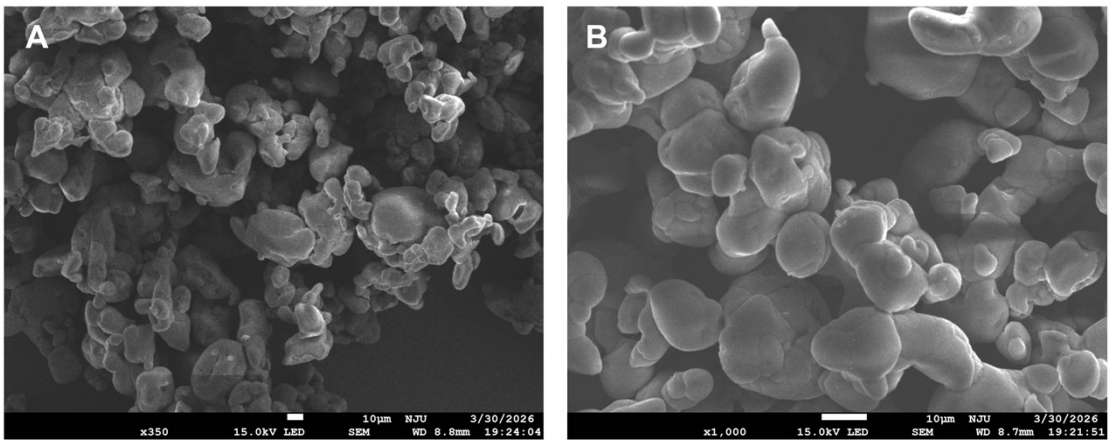

Fig. S5. SEM images of sulfur produced by H_2S oxidation reaction in EmimAc.

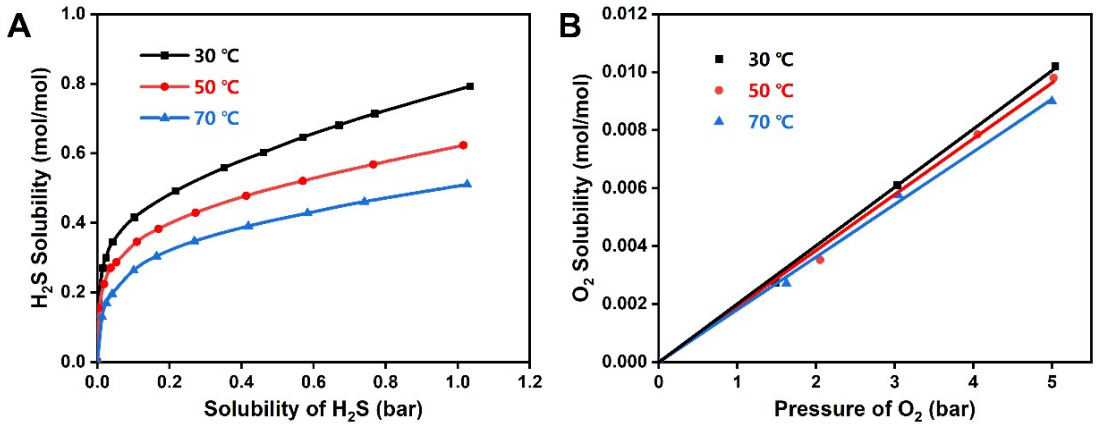

Fig. S6. Solubility of H_2S (A) and O_2 (B) in EmimAc at different temperatures.

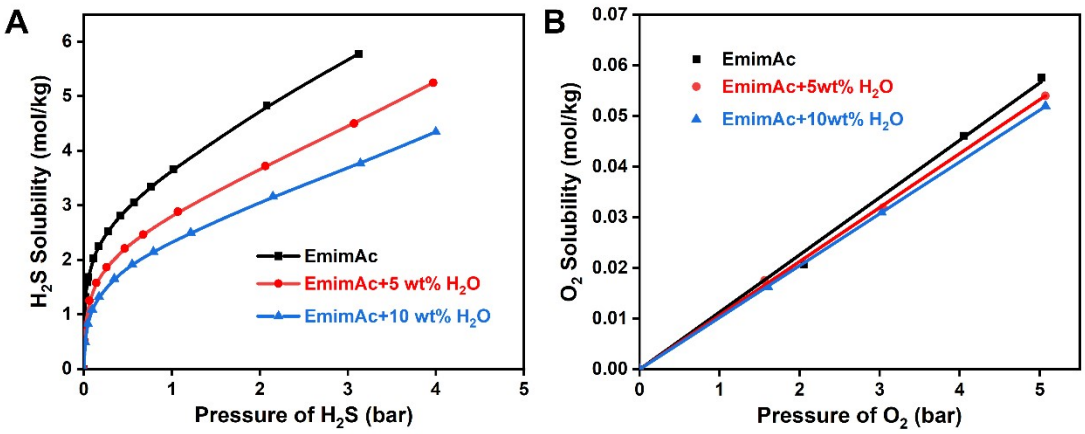

Fig. S7. Solubility of H_2S (A) and O_2 (B) in EmimAc containing varying water contents.

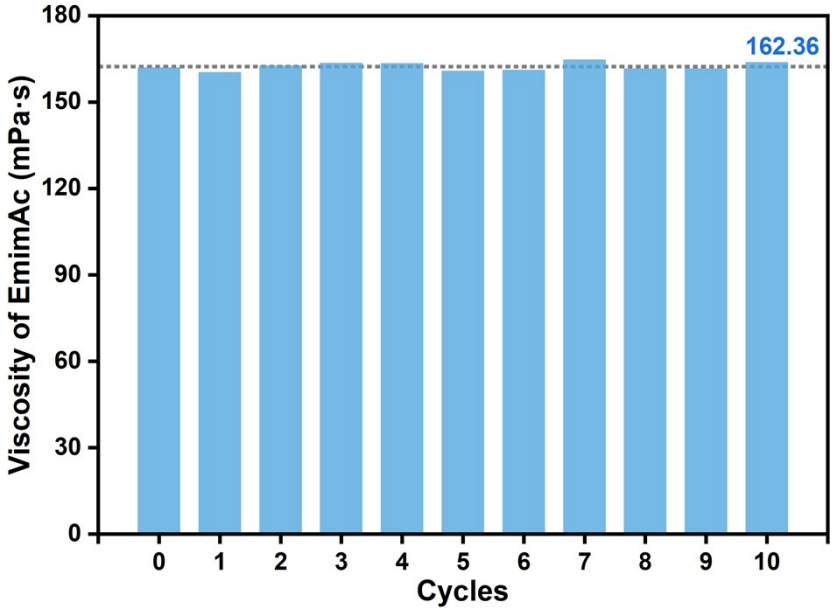

Fig. S8. Viscosity of EmimAc over ten consecutive cycles (25 °C).

4. Tables S1 to S7.

Table S1. Names, abbreviations, purities and suppliers of reagents used in this work.

Names	Abbreviations	Purities	Suppliers
1-Ethyl-3-methylimidazole acetate	EmimAc	98%	Shanghai Chengjie Chemical Co., Ltd.
1-Butyl-3-methylimidazolium acetate	BmimAc	98%	Shanghai Chengjie Chemical Co., Ltd.
1-Hexyl-3-methylimidazolium acetate	HmimAc	98%	Shanghai Chengjie Chemical Co., Ltd.
1-Ethyl-3-methylimidazolium trifluoroacetate	EmimTFA	98%	Shanghai Aladdin Reagent Co., Ltd.
1-Hexyl-3-methylimidazolium chloride	HmimCl	99%	Shanghai Titan Technology Co., Ltd.
1-Hexyl-3-methylimidazolium bis(trifluoromethanesulfonyl)imide	$HmimTf_2N$	98%	Shanghai Meryer Biochemical Technology Co., Ltd.
1-Hexyl-3-methylimidazolium hexafluorophosphate	$HmimPF_6$	99%	Shanghai Titan Technology Co., Ltd.
1-Hexyl-3-methylimidazolium tetrafluoroborate	$HmimBF_4$	99%	Shanghai Titan Technology Co., Ltd.
1,8-Diazabicyclo[5.4.0]undecane-7-ene	DBU	99%	Shanghai Meryer Biochemical Technology Co., Ltd.
Imidazole	Im	99%	Shanghai Aladdin Reagent Co., Ltd.
Tetraethylammonium hydroxide	$N_{2222}OH$	AR, 25% in water	Shanghai Aladdin Reagent Co., Ltd.
Acetic acid	HAc	99.5%	Shanghai Aladdin Reagent Co., Ltd.
Lactic acid	HL	AR	Shanghai Meryer Biochemical Technology Co., Ltd.
Ethanol	-	99.7%	Shanghai Titan Technology Co., Ltd.

Table S2. The elemental analysis results of sulfur produced by H_2S oxidation reaction in EmimAc.

N (%)	C (%)	H (%)	S (%)
0.088	0.675	0.194	97.281

Table S3. Expressions obtained by correlation of solubility data of H_2S and O_2 in different ILs (x and y represent the pressure of H_2S and O_2 in bar, respectively) [a].

Entries	Solvents	T(℃)	Solubility of H_2S		Expressions for the solubility of O_2
			Expressions	Fitting methods	
1	H_2O	50	0.05837*x	Linear fitting	9.406E-04*y
2	EmimAc	50	(4*4.17896*x*1000/170.21+1-(8*1000/170.21*4.17896*x+1)^0.5)/(8*4.17896*x)+x/0.91445	RETM2:1	0.01131*y
3	BmimAc	50	(4*7.64949*x*1000/198.27+1-(8*1000/198.27*7.64949*x+1)^0.5)/(8*7.64949*x)+x/0.82779	RETM2:1	0.01056*y
4	HmimAc	50	(4*11.70683*x*1000/226.32+1-(8*1000/226.32*11.70683*x+1)^0.5)/(8*11.70683*x)+x/0.85291	RETM2:1	0.009798*y
5	N_{2222}Ac	50	(4*2.02392*x*1000/189.3+1-(8*1000/189.3*2.02392*x+1)^0.5)/(8*2.02392*x)+x/2.14193	RETM2:1	0.008616*y
6	N_{2222}L	50	(4*0.47317*x*1000/219.33+1-(8*1000/219.33*0.47317*x+1)^0.5)/(8*0.47317*x)+x/3.79577	RETM2:1	0.006434*y
7	EmimTFA	50	0.3046*x	Linear fitting	0.01840*y
8	HmimCl	50	(4*0.04574*x*1000/202.73+1-(8*1000/202.73*0.04574*x+1)^0.5)/(8*0.04574*x)+x/1.36987	RETM2:1	0.01049*y
9	[DBUH]Im	50	(1000/220.32)*428.16952*x/(428.16952*x+1)+x/1.19091	RETM1:1	N.A.[b]
10	EmimAc	30	(4*13.28577*x*1000/170.21+1-(8*1000/170.21*13.28577*x+1)^0.5)/(8*13.28577*x)+x/0.52415	RETM2:1	0.01181*y
11	EmimAc	70	(4*1.53881*x*1000/170.21+1-(8*1000/170.21*1.53881*x+1)^0.5)/(8*1.53881*x)+x/1.56622	RETM2:1	0.01065*y
12	EmimAc+5 wt% H_2O	50	(4*1.12189*x*1000/170.21+1-(8*1000/170.21*1.12189*x+1)^0.5)/(8*1.12189*x)+x/1.73996	RETM2:1	0.01065*y
13	EmimAc+10 wt% H_2O	50	(4*0.59185*x*1000/170.21+1-(8*1000/170.21*0.59185*x+1)^0.5)/(8*0.59185*x)+x/3.10183	RETM2:1	0.01024*y

[a] The units of the solubility data are in terms of mol/kg.

[b]The solubility of O_2 in [DBUH]Im could not be measured.

Table S4. Results of H_2S oxidation reactions in different ILs[a].

Entries	Solvents	T (℃)	H_2S:O_2 (mmol)	Conversion rate of H_2S (%)[b]	Sulfur recovery rate (%)
1	H_2O[c]	50	6:3	5.6	4.4
2	EmimAc	50	6:3	96.1	94.3
3	BmimAc	50	6:3	95.8	92.5
4	HmimAc	50	6:3	95.6	93.2
5	N_{2222}Ac	50	6:3	83.7	81.5
6	N_{2222}L	50	6:3	71.9	70.2
7	EmimTFA	50	6:3	19.9	18
8	HmimCl	50	6:3	12.1	11.5
9	HmimTf_2N	50	6:3	N.D.[d]	N.D.
10	HmimPF_6	50	6:3	N.D.	N.D.
11	HmimBF_4	50	6:3	N.D.	N.D.
12	[DBUH]Im	50	6:3	46.4[e]	N.D.
13	EmimAc[f]	50	6:3	84.7	80.1
14	EmimAc[g]	50	6:3	97.2	94.9
15	EmimAc	50	6:2	61.0	57.4
16	EmimAc	50	6:4.5	97.9	95.2
17	EmimAc	30	6:3	62.7	60.5
18	EmimAc	70	6:3	93.8	88.7
19	EmimAc+5wt%H_2O	50	6:3	81.5	78.9
20	EmimAc+10wt%H_2O	50	6:3	65.8	63.1

[a] Reaction conditions: The amount of IL used was 6 mmol. The quantities of H_2S and O_2 introduced into the reactor were 6 mmol and 3 mmol, respectively, with a reaction duration of 3 h at 50°C.

[b] The H_2S conversion rate was calculated by dividing the amount of H_2S consumed during the reaction by the initial total amount of H_2S introduced.

[c] The mass of H_2O used in the reaction system was 1.0 g.

[d] N.D.: No elemental sulfur was observed to form following the completion of the reaction.

[e] Since the solubility of O_2 in [DBUH]Im was not determined, only the solubility of H_2S therein was considered when calculating the H_2S conversion rate.

[f] The amount of EmimAc used in the reaction system was 3 mmol.

[g] The amount of EmimAc used in the reaction system was 9 mmol.

Table S5. Cartesian coordinates of EmimAc+H_2S complex from Gaussian 16 program.

Atoms	Coordinates (Angstroms)		
	X	Y	Z
O	2.2639	-1.448547	-0.031558
C	1.333616	-1.444899	-0.873495
C	0.731026	-2.787863	-1.287115
O	0.858928	-0.414185	-1.445947
H	0.773585	-3.510764	-0.470015
H	-0.299157	-2.67893	-1.630637
H	1.318809	-3.193825	-2.118107
C	-0.880477	0.92378	1.048649
N	-1.912172	0.30857	0.465203
C	-1.85489	-1.038889	0.771412
C	-0.765564	-1.219837	1.565788
N	-0.175432	0.019239	1.729902
C	-2.903548	0.946648	-0.417037
C	-2.616822	0.673993	-1.885243
C	1.065595	0.275799	2.458661
H	-0.643339	1.97011	0.967689
H	-2.587053	-1.735937	0.400768
H	-0.356286	-2.104635	2.022262
H	-3.88222	0.56571	-0.123397
H	-2.879659	2.01391	-0.198524
H	-3.391095	1.145461	-2.495631
H	-1.64799	1.08038	-2.180215
H	-2.619428	-0.397307	-2.098068
H	1.89138	-0.163843	1.90099
H	1.200764	1.350171	2.553919
H	0.994572	-0.171289	3.449322
S	2.042399	2.346084	-0.691259
H	2.881813	1.864735	0.250803
H	1.543908	1.063508	-1.006417

Table S6. Cartesian coordinates of H_2O+H_2S complex from Gaussian 16 program.

Atoms	Coordinates (Angstroms)		
	X	**Y**	**Z**
O	2.246512	0.11336	0.040481
H	1.285168	-0.015699	-0.007746
H	2.640792	-0.72118	-0.242346
S	-1.191494	-0.096355	-0.0533
H	-1.423069	1.169149	-0.467151
H	-1.411086	0.202528	1.246193

Table S7. Cartesian coordinates of EmimAc+O_2 complex from Gaussian 16 program.

Atoms	Coordinates (Angstroms)		
	X	Y	Z
O	-2.732999	1.671736	-0.04783
C	-1.592692	1.683371	0.495116
C	-1.539298	1.437386	2.009496
O	-0.498364	1.909057	-0.089315
H	-2.345243	0.778902	2.339907
H	-0.577633	1.02247	2.316494
H	-1.666353	2.396966	2.523988
C	0.168647	-1.073967	-0.976628
N	0.515041	-1.545684	0.223569
C	-0.634018	-1.904837	0.905497
C	-1.683071	-1.644076	0.079602
N	-1.158019	-1.132934	-1.092264
C	1.88583	-1.604648	0.756671
C	2.126544	-0.541431	1.816782
C	-1.937086	-0.635936	-2.225153
H	0.846853	-0.694103	-1.720538
H	-0.599664	-2.307542	1.903364
H	-2.743912	-1.766426	0.216822
H	2.03398	-2.608569	1.156617
H	2.556723	-1.481707	-0.092416
H	3.16584	-0.595564	2.150157
H	1.94041	0.458584	1.422148
H	1.484668	-0.69592	2.686925
H	-2.46727	0.262272	-1.909858
H	-1.256578	-0.401589	-3.040568
H	-2.638328	-1.406421	-2.54279
O	3.135909	1.959944	-0.824815
O	3.345231	0.895989	-1.350251

Table S8. Cartesian coordinates of H_2O+O_2 complex from Gaussian 16 program.

Atoms	Coordinates (Angstroms)		
	X	Y	Z
O	-2.507345	-0.120294	-0.000163
H	-1.553002	-0.266685	0.001931
H	-2.623439	0.838241	-0.00532
O	2.102675	-0.105254	-0.001974
O	0.926725	0.154103	0.00256

5. References

1. M. O. M. W. Lemmon, D.G. Friend, NIST ChemistryWebBook, NIST Standard Reference Database Number 69, National Institute of Standards and Technology, Gaithersburg MD, 2018.
2. X. M. Zhang, W. J. Xiong, L. L. Peng, Y. T. Wu and X. B. Hu, *AIChE J.*, 2020, **66**, e16936.